International Journal of Food Microbiology 292 (2019) 21–30

Contents lists available at ScienceDirect

International Journal of Food Microbiology

journal homepage: www.elsevier.com/locate/ijfoodmicro

Antibacterial properties of nanofibers containing chrysanthemum essential oil and their application as beef packaging

Lin Lin[a], Xuefang Mao[a], Yanhui Sun[b], Govindan Rajivgandhi[a], Haiying Cui[a,*]

[a] School of Food and Biological Engineering, Jiangsu University, Zhenjiang 212013, China
[b] School of Biological Science and Food Engineering, Chuzhou University, Chuzhou 239000, China

ARTICLE INFO

Keywords:
Chrysanthemum essential oil
Nanofibers
L. monocytogenes
Antibacterial mechanism

ABSTRACT

This study was aimed to develop novel antibacterial packaging materials in order to reduce the microbial contamination of food surface. Chrysanthemum essential oil (CHEO) was successfully incorporated into chitosan nanofibers (CS/NF) through electrospinning which was demonstrated by SEM and AFM analysis. The antibacterial mechanism of CHEO against *Listeria monocytogenes* (*L. monocytogenes*) was explored as well. The cell membrane permeability of *L. monocytogenes* appeared to be increased by CHEO. In addition, respiratory metabolism of *L. monocytogenes* was inhibited by CHEO through the inhibition of the Embden-Meyerhof-Parnas (EMP) pathway. The presence of CHEO had a negative effect on the activity of hexokinase, phosphofructokinase and pyruvate kinase in *L. monocytogenes* cells. Release efficiency study indicated that the CHEO could be released slowly from CHEO/CS/NF to achieve long-lasting antibacterial effect. The antibacterial application of the CHEO nanofibers against *L. monocytogenes* was tested on beef, with an inhibition rate of 99.91%, 99.97%, and 99.95% at the temperature of 4 °C, 12 °C and 25 °C, respectively, after 7 days of storage. Beef parameters like thiobarbituric acid reactive substances (TBARS), pH values, and texture at different storage temperatures (4 °C, 12 °C and 25 °C) were evaluated as well. Due to the presence of antioxidant components in CHEO released from CHEO/CS/NF, the TBARS value in treated beef was 0.135 MDA/kg lower ($P < 0.05$) than the untreated sample at 4 °C after 12 days. PH value assay indicated that PH value of beef sample packed with CHEO/CS/NF (6.43) was lower than unpacked sample (7.05) at 4 °C after 10 days of storage. These obtained results all illustrated the fact that CHEO/CS/NF could prolong the shelf-life of beef, suggesting a potential application in food packaging.

1. Introduction

L. monocytogenes is one of the most important spoilage microorganisms in meat products (Tsigarida et al., 2010). It can survive in refrigeration condition and tolerate relatively low PH and high concentration of salt (Wemmenhove et al., 2016). When the food contaminated with *L. monocytogenes* is ingested by consumers, it will lead to sepsis, meningitis and the spontaneous abortions in pregnant women (Vodnar, 2012). Especially, meats including beef are natural mediums for *L. monocytogenes*, because they are rich in protein, fat and moisture. In consequence, there is a critical demand in food safety for seeking effective antibacterial agents to eliminate *L. monocytogenes* in meat products. As botanical extracts, essential oils attracted new interest in substitution for other antibacterial additives due to their high antibacterial activities and non-toxic (Gutierrez et al., 2008; Pesavento et al., 2015).

Chrysanthemum essential oil (CHEO) is aromatic oily liquid extracted from chrysanthemum. Chrysanthemum is a perennial herb belonging to Asteraceae, which can prevent various diseases, such as hypertension, coronary heart disease and arteriosclerosis (Khallouki et al., 2000). Some previous studies reported that CHEO has antibacterial, antifungal, immunomodulatory, anti-inflammatory, and antirheumatic activities (Arokiyaraj et al., 2014). Few reports mentioned the antibacterial activity and antibacterial mechanism of CHEO. Only limited researches are available on food preservation by CHEO due to its sensitivity to air, humidity and high temperature (Catanzano et al., 2015). Therefore, it is necessary to improve the stability of CHEO before it can be applied in food industry.

Encapsulation technology is widely used to enclose active substances inside a micrometric wall made of hard or soft soluble film, which can increase the stability of the active substances being encapsulated. In recent years, many different methods were developed to encapsulate essential oils and enhance their stability. Among them, nanofibers (NF) performed considerable attentions. Compared to other

* Corresponding author.
E-mail address: cuihaiying@ujs.edu.cn (H. Cui).

https://doi.org/10.1016/j.ijfoodmicro.2018.12.007
Received 11 May 2018; Received in revised form 3 December 2018; Accepted 6 December 2018
Available online 08 December 2018

methods, nanofibers possess the merits of high surface area, easy encapsulation of active agents, high encapsulation efficiency and nanoporous features (Rieger, 2013). As new active food packaging material, it can prolong shelf-life and keep nutrients of food intact (Brown et al., 2016; Huang et al., 2003). The key to fabricate the essential oil/nanofibers is to find an appropriate substrate material with good biocompatibility and spinnability.

Chitosan (CS) is a natural biopolymer obtained from partial or total deacetylation of chitin. Some literatures verified that CS can be utilized as a carrier to encapsulate active ingredients and improve their stability (Ammar et al., 2012; Haider and Park, 2009). In the present study, chitosan (CS) was selected as a substrate material for electrospinning because of its high biodegradability, high biocompatibility and spinnability (Krauland and Alonso, 2007; Lasheen et al., 2016).

As a proof of concept, the CHEO/CS/NF was prepared by electrospinning and its application as a beef packaging material was evaluated. Meanwhile, its possible antibacterial mechanism was explored as well. Additionally, the quality parameters of beef after CHEO/CS/NF treatment, including TBARS value, pH value, color and texture evaluation, were also monitored.

2. Materials and methods

2.1. Materials and culture

CHEO was provided by Chuzhou University, and it was called “chuju” which was grown in Chuzhou, China. Its Voucher number is CM28. CHEO was extracted from chrysanthemum through carbon dioxide supercritical extraction (Caredda et al., 2002). Polyethylene oxide (PEO, average Mv~900000) was purchased from Sigma-Aldrich Chemical Co. (St. Louis, Mo, USA). CS was purchased from Sinopharm Chemical Reagent Co., Ltd. (Shanghai, China). The strain of *Listeria monocytogenes* ATCC 19115 was provided by Food and Biological Engineering, Jiangsu University. The strain was shaking cultured in nutrient broth peptone yeast extract-glucose (PYG) at 37 °C for 48 h. PYG was made of yeast extract, peptone, glucose and agar, the materials were purchased from Sinopharm Chemical Reagent Co., Ltd. (Shanghai, China). Fresh beef was purchased from the local supermarket.

2.2. Determination of CHEO

2.2.1. Analysis of chemical compositions of CHEO

The chemical compositions of CHEO were analyzed by gas chromatographemass spectrometer (GC–MS, Agilent 6890GC/5973NFSD, NYSE: A, USA). The components were separated using a fused silica capillary Agilent Technology HP-5 ms (5% phenyl methyl siloxane) column (30 m × 0.25 mm × 0.25 μm, film thickness 0.1 μm). The injector temperature was 250 °C. The initial temperature of the column was 50 °C for 1 min, then programmed at rate of 10 to 200 °C/min and held for 2 min. Afterwards, the temperature was raised to 220 °C at 5 °C/min, kept for 10 min. One microliter samples were injected in the split ratio of 10:1 (Cui et al., 2018).

2.2.2. Determination of minimum inhibitory concentration (MIC)

A two-fold serial dilution method was used to determine the MIC of CHEO. CHEO dissolved in absolute ethanol was added into tube containing sterile PYG and a series of concentration of CHEO ranged from 0.625 to 5.0 mg/mL was diluted. Subsequently, *L. monocytogenes* was transferred to each tube to obtain bacteria concentration of 10^4–10^5 CFU/mL. The tubes were incubated at 37 °C with oscillation for 48 h. The minimum concentration of CHEO that did not exhibit any visible growth of bacteria was defined as MIC.

2.2.3. Time-kill analysis of CHEO

The anti-bacterial activity of CHEO was tested by the method of plate colony counting. CHEO was dissolved in absolute ethanol and diluted into tubes containing *L. monocytogenes* (10^5–10^6 CFU/mL) to obtain the concentration of 1.25 mg/mL, 2.5 mg/mL, and 5 mg/mL whereas the without addition of CHEO in the PBS containing bacterial culture acted as a negative control and with only absolute ethanol (0.125%, 0.25%, 0.5%) in the PBS containing bacterial culture acted as positive controls. Then the samples were incubated with 120 rpm at 37 °C for 48 h. All measurement was repeated 3 times to ensure the accuracy value. And the reduction in population (P %) of bacteria was calculated by the following equations:

$$P\% = \frac{\text{population of control bacteria} - \text{population of experimental bacteria}}{\text{population of control bacteria}} \times 100\%$$

2.2.4. Transmission Electron Microscopy (TEM) analysis

The minimum inhibitory concentration (MIC) of CHEO was added to test tubes containing *L. monocytogenes* (10^8–10^9 CFU/mL), and without addition of CHEO containing *L. monocytogene* tubes were taken for TEM analysis. After 24 h incubation, the bacteria samples were centrifuged at 6000 rpm for 10 min at 4 °C and washed thrice with 0.03 M PBS (pH 7.2). The copper screen was in touch with the bacterial suspension for 3 min and dried. Then, the copper screen was dyed with 3% (vol/vol) phosphotungstic acid for 3 min and dried, followed by microscopic examination (JEM-2100, JEOL, Tokyo, Japan).

2.2.5. The bactericidal mechanism of CHEO

The possible antibacterial mechanisms of CHEO against *L. monocytogenes* were explored. The MIC concentration of CHEO treated (2 h) and untreated samples were used for this study. After 2 h incubation, the samples were centrifuged at 4000 rpm for 15 min to obtain the supernatants which were diluted 20 times with distilled water. The conductivity was determined by a conductivity meter. All assays were performed in triplicate. The conductivity rate formula is as follows:

$$R(\%) = \frac{Rs\text{-}Rc}{Rc} \times 100\%$$

where R represented the conductivity change rate, Rs and Rc represented the conductivity rate of experimental group and control group.

Moreover, the bacteria solution treated with CHEO (MIC) was washed twice with 1 mM KNO_3 (pH 6.2) solution, then the surface potential of bacteria was measured by Zeta potential analyzer at room temperature.

Cell-surface hydrophobicity referred to the unstable state of bacteria in polar water, which caused a series of changes in the rearrangement and arrangement of cells. The surface hydrophobicity of *L. monocytogenes* was expressed by the bacterial adsorption rate which was determined by microbial adhesion to hydrocarbons (MATH). The cultured bacteria were centrifuged and resuspended in 0.1 mol/L $KN0_3$ (pH 6.2) solution to OD_{600} = 0.2. A test tube containing 4 mL of bacterial suspension, CHEO (MIC) and 1.5 mL of hexadecane (organic phase) was mixed and incubated for 15 min at room temperature to separate two phases. Afterwards, the absorbance of aqueous phase at 600 nm was measured. The formula of bacterial adsorption rate was as follows:

$$BA\ (\%) = \frac{OD_0 - OD_1}{OD_0} \times 100\%$$

BA referred to the bacterial adsorption rate, OD_1 was the OD_{600} of the experimental group and OD_0 was the OD_{600} of the control group respectively. All assays were performed in triplicate.

The cell membrane permeability was determined by cellular β-galactosidase. After induction of β-galactosidase, 900 μL of *L. monocytogenes* reaction buffer was mixed with 100 μL of 1 mg/mL ONPG and CHEO (MIC) at 37 °C in water bath. After 3 h, the OD was measured at 405 nm using UV spectrophotometer (NANODROP 2000, Thermo Fisher Scientific, Waltham, MA, USA), and the control sample was also

measured at 405 nm. The D-value (OD = OD_t-OD_0) can reflect the increase of *L. monocytogenes* membrane permeability.

The loss of cellular absorbing material in the MIC of CHEO treated bacterial culture was analyzed at 260 nm using UV spectrometer.

The genomic DNA of CHEO (MIC) treated *L. monocytogenes* was extracted using TIANamp Bacterial DNA Kit (TIANGEN Biotechnology, Beijing, China). The protein concentration was tested by the BCA kit (Jiancheng Bioengineering Institute, Jiangsu, China) using the bicinchoninic acid method and the cellular ATP concentration was determined by the Clean SenseTM Surface Hygiene Test Kit (LEYU Biotechnology, Shanghai, China), which is based on the detection of light generated by the ATP-dependent enzymatic conversion of D-luciferin to oxyluciferin by firefly luciferase (Cui et al., 2016).

2.2.6. Effects of CHEO on respiratory metabolism of L. monocytogenes

The respiration rate refers to the amount of oxygen consumed by microorganisms per unit mass. The respiration rate could be calculated on the basis of the change of dissolved oxygen in the solution. 3.6 mL PBS (0.03 M, pH 7.3), 0.4 mL glucose solution and 1.0 mL *L. monocytogenes* suspension (10^6 CFU/mL) were added to a tube which was exposed to the air for 5 min. Then the dissolved oxygen meter was used to determine the dissolved oxygen content in the suspension in a sealed condition, before the initial respiration rate R_0 was calculated based on the dissolved oxygen content. The amounts of dissolved oxygen of three typical inhibitors (malonic acid, iodoacetic acid and sodium phosphate, 500 mg/L) and CHEO (MIC) in the solutions were measured by the same method respectively, which was calculated as respiration rate R_1 (Benker, 1985; Schmidt and Dringen, 2009) Afterwards, the contents of dissolved oxygen of the suspension containing both typical inhibitor and CHEO (½ MIC) are determined, the respiration rate R_2 was calculated. The respiratory rate of inhibition I_R and respiratory superpose rate D_R was determined as follows:

$$I_R = \frac{R_0\text{-}R_1}{R_0} \times 100\%$$

$$D_R = \frac{R_1\text{-}R_2}{R_1} \times 100\%$$

2.2.7. The activity of three enzymes in the EMP pathway of L. monocytogenes

The activity of Hexokinase (HK), phosphofructokinase (PFK), and pyruvate kinase (PK) in EMP pathway of *L. monocytogenes* was tested by HK Assay Kit, PFK Assay Kit and PK Assay Kit (Keming Bioengineering Institute, Jiangsu, China).

2.3. Preparation of electrospinning nanofibers

0.45 g (1.5% w/v) chitosan was dissolved in 30 mL deionized water containing 1% (v/v) glacial acetic acid under magnetic stirring at 50 °C for 30 min, afterwards, 1.5% (w/v) PEO and CHEO (2MIC, 150 mg) were added to the above solution respectively and continuously magnetic stirring for 24 h in room temperature to obtain the homogeneous electrospinning solution. The final solution was subjected to electrospinning (SNAN-01, MECC Co., Ltd., Fukuoka, Japan) through a 5.0 mL polypropylene syringe with an injection needle with 0.5 mm inner diameter. Electrospinning was performed by the impressed voltage at 25 kV with a power supply. The flow rate of the spinning solution was controlled at 0.2 mL/h driven by a syringe pump. The vertical distance was 15 cm between the needle tip and the collector where aluminum foil was put to gather fibers. For comparison, the solution without CHEO was prepared and the nanofibers were obtained through electrospinning (Cui et al., 2017). The morphology and nanofibers diameter were observed by SEM.

2.4. Characterization of electrospinning nanofibers

2.4.1. Atomic Force Microscopy (AFM) analysis

The surface topography and the surface roughness information could be obtained with nanometer resolution using an AFM (Multimode 8, Bruker Co., Massachusetts, USA). The surface of the nanofiber membranes was scanned by an extremely sharp tip and the sensor was used to detect the changes to get the force distribution information (Alippilakkotte and Sreejith, 2018).

2.4.2. Physical properties of the nanofibers

An electronic digital micrometer (accuracy 0.001 mm, Guangdong, China) was used to detect the film thickness. All the samples were performed ten times. Average values were calculated with an accuracy of 0.002 mm.

The nanofibers (1 cm × 1 cm) was weighed and dried at 120 °C to obtain a constant weight. The moisture content of the film was calculated according the following formula:

$$\text{Water content} = \frac{M_0 - M_i}{M_0} \times 100\%$$

M_0 and M_i are the mass of initial and dried samples (mg), respectively (Shojaeealiabadi et al., 2013). All the samples were performed in triplicate.

Films (1 cm × 1 cm) were dried at 120 °C until achieving a constant weight and weighed them. Then the samples were added in 10 mL distilled water. After immersion for 24 h, undissolved film pieces were taken out and dried at 120 °C until constant weight to determine the final weight. The water solubility was calculated according the following equation:

$$\text{Water solubility} = \frac{W_0 - W_i}{W_0} \times 100\%$$

W_0 and W_i represent the mass of initial and dried samples (mg) (Samira et al., 2014). All the samples were performed in triplicate.

Transparency of the film was measured using a spectrophotometer at the wavelength of 600 nm (Shimadzu, model UV-160, Kyoto, Japan). The film sample was cut into a size (50 mm × 4 mm) and placed inside the plastic cuvette. Transparency of the films was calculated as follow:

$$T = \frac{-\log T_{600}}{X}$$

where T_{600} is the transmittance of light through the film at 600 nm, X is the film thickness (mm). All samples were performed in triplicate (Ubonrat and Brucer, 2010).

2.5. Release rate of nanofiber membranes in vitro

10 g of CHEO/CS/NF was added to 10 mL absolute ethanol treated by ultrasonic (100 W, 20 °C) for 3 h. Subsequently, the sample was centrifuged at 6000 rpm for 20 min to obtain the supernatant solution. In order to estimate the concentration of CHEO released from the nanofiber, the solution was analyzed by GC–MS. The same quality of CHEO/CS/NF was added to 10 mL absolute ethanol and cultured at 4 °C, 12 °C, 25 °C for 15 days. During the period, a certain amount of supernatant solution was removed at the predetermined time intervals to determine the concentration of CHEO analyzed by GC–MS. The release rate of CHEO in CHEO/CS/NF was calculated by the following formula:

$$RR\ (\%) = \frac{W_{release}}{W_{total}} \times 100\%$$

where RR was the release rate (%), $W_{release}$ (mg/mL) meant the amount of CHEO released from nanofiber membranes after incubation for a period of time, and W_{total} (mg/mL) was the total amount of CHEO in nanofiber membranes.

2.6. Antibacterial application of electrospun nanofilm on beef in vitro

The experiment was conducted by packing fresh beef (1.5 cm × 1.5 cm × 1.0 cm) with the antibacterial nanofiber membranes (5 cm × 5 cm). Before packing, the beef was soaked in the prepared bacteria solution of *L. monocytogenes* (approximately 10^2–10^3 CFU/mL) and dried for 30 min in sterile environment. There were three treatments, one was packed with CHEO/CS/NF, another was packed with CS/NF used as negative control and the beef packed with only sterile aluminized paper was employed as control. The samples were placed at 4, 12, and 25 °C for 7 days. One piece of beef sample was added to sterile PBS and shaken in a homogenizer for 30 min. Then the plate count method was used to obtain the number of residual bacteria every day. The experiments were performed in triplicate.

2.7. TBARS and pH value of beef

The TBARS values of beef samples were measured using the method described by Zhang et al., 2016. Beef samples with or without treatment of CHEO/CS/NF were used for TBARS evaluation after storing at the temperature of 4 °C for 12 days, 12 °C for 8 days and 25 °C for 4 days. 10 g beef sample was added to 50 mL 20% trichloroacetic acid (containing 2 M phosphoric acid) and homogenized at 10000 rpm for 30 s. Then the homogenate was filtered to obtain the filtrate (1 mL) which was heated in boiling water bath for 30 min. Afterwards, the filtrate was analyzed by an ultraviolet spectrophotometer, and the absorption peak of measured material was at 534 nm. The standard calibration curve was determined by 1, 1, 3, 3-tetraethoxypropane.

PH value of beef sample was evaluated to know the change of beef quality after treatment. The samples (10 g) were homogenized with 90.0 mL distilled water and then filtered with sterile gauze (Miao et al., 2015). PH was measured using a digital pH meter (FE20K, METTLER TOLEDO, Zurich, Switzerland).

2.8. Color and texture evaluation

In order to comprehensively understand the quality of the beef treated with nanofibers, fresh beef samples treated with CHEO/CS/NF were used for evaluation after storing at the temperature of 4 °C for 7 days and 25 °C for 3 days. The beef samples packed with blank sterile aluminized paper were employed as control.

Within a certain time interval, the changes of beef surface color were determined by a Chromatic meter (Color Quest XE, Hunter Lab Co., Reston, Virginia, USA). The color was evaluated by L*, a*, and b*.

In addition, surface texture measurement of the beef was performed using a TA.XT. Plus (Stable Micro Systems Ltd., Godalming, Surrey, UK). The texture quality of each beef sample was examined through hardness, adhesiveness, resilience, cohesion, springiness, gumminess and chewiness. The beef samples were compressed twice at test speed of 2.00 mm/s, strain of 50% and trigger force of 5.0 g (Lin et al., 2017).

2.9. Statistical analysis

SPSS software (version 22.0; IBM Corp., Armonk, NY) and origin 8.6.0.0 were used to analyze the data of the studies. A one-way analysis of variance (ANOVA) and the Bonferroni statistical test were used to determine significant differences at a significance level of $P < 0.05$. The error bars are presented as means ± standard deviations (SD). All experiments were performed in triplicate.

3. Results and discussion

3.1. Determination of CHEO

3.1.1. Analysis of chemical compositions of CHEO

As shown in Table 1, the main 12 chemical compositions of CHEO were listed as follows: borneol (19.55%), β-Selinene (16.25%), camphor (13.48%), Guaia-3, 9-diene (5.26%), Hexaoxa-cyclooctadecane (4.16%), Cyclopropa-naphthalene (2.69%), 1,4,7,10,13,16-Hexaoxacyclooctadecane (2.33%), 3-ethylidence-1-methylcyclopentene (1.88%), A-Curcumene (1.25%), eucalyptol (1.11%), Pentanoic acid (1.05%), 1,4,7,10,13,16-Hexaoxacyclooctadecane (0.92%), 1-Phenyl-2-propanol (0.63%), Octaethylene glycol (0.56%), 3,6,9,12,15-Pentaoxanonadecan-1-ol (0.27%).

3.1.2. MIC and Time-kill analysis of CHEO

The MIC (2.5 mg/mL) was obtained through two-fold serial dilution method. The antibacterial activity of CHEO against *L. monocytogenes* was displayed in Fig. 1A. The initial concentration of *L. monocytogenes* was 6.5 log CFU/mL. Compared with control group, the population of bacteria was reduced respectively to 3.9 log CFU/mL, 2.8 log CFU/mL, 0 log CFU/mL after treating with 1/2 MIC, MIC and 2 MIC of CHEO for 4 h (Lin et al., 2016). The results indicated CHEO had strong antibacterial activity against *L. monocytogenes*. Khallouki et al. (2000) also reported the same function of CHEO.

3.1.3. TEM analysis

The morphological changes of *L. monocytogenes* were observed through TEM (Fig. 1B and C). The untreated *L. monocytogenes* showed a typical cell structure with regular shape and a smooth wall, while the cells treated with CHEO was deformed with destroyed membrane. The phenomenon implied that CHEO could lead to irreversible destructions on *L. monocytogenes* membrane.

3.1.4. The bactericidal mechanism of CHEO

The inhibition bacterial mechanism was given in Table 2, the results suggested that the CHEO might increase membrane permeability by destroying the cell membrane, causing the leakage of cellular substances. The quantification of DNA, protein, and ATP in *L. monocytogenes* was reduced by 73.58%, 70.01%, and 84.63%, respectively, as compared with the control group. Obviously, the loss of cellular materials was attributed to the breakage of membrane, this conclusion was

Table 1
The chemical compositions of CHEO.

Composition	Proportion (%)	Composition	Proportion (%)
Borneol	19.55 ± 0.031	α-Curcumene	1.25 ± 0.021
β-Selinene	16.25 ± 0.052	Eucalyptol	1.11 ± 0.013
Camphor	13.48 ± 0.021	Pentanoic acid	1.05 ± 0.018
Guaia-3,9-diene	5.26 ± 0.019	Butanoic acid, 3-methyl-,1,7,7-trimethylbicyclo[2.2.1]hept-2-yl ester	1.0 ± 0.007
Hexaoxa-cyclooctadecane	4.16 ± 0.012	1,4,7,10,13,16-Hexaoxacyclooctadecane	0.92 ± 0.011
Cyclopropa-naphthalene	2.69 ± 0.015	3-Cyclohexene-1-methanol, alpha., alpha., 4-trimethyl	0.92 ± 0.003
1,4,7,10,13,16-Hexaoxacyclooctadecane	2.33 ± 0.004	1-Phenyl-2-propanol	0.63 ± 0.011
3-ethylidence-1-methylcyclopentene	1.88 ± 0.008	Octaethylene glycol	0.56 ± 0.042
Tetramethyl-undeca-2,6,9-trien-8-one	1.42 ± 0.014	3,6,9,12,15-Pentaoxanonadecan-1-ol	0.27 ± 0.026

Values are expressed as mean ± SD.

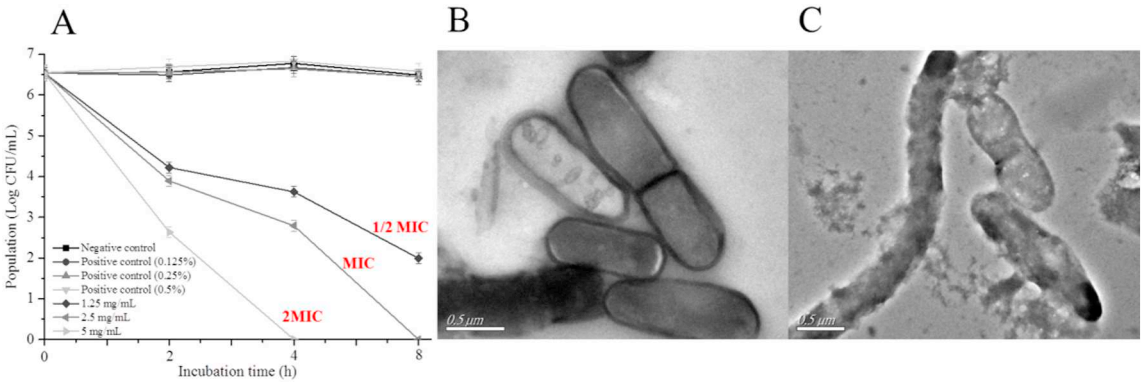

Fig. 1. The antibacterial activity of CHEO against *L. monocytogenes*, (A) Time-kill curve of CHEO against *L. monocytogenes*, TEM images of (B) *L. monocytogenes*, (C) *L. monocytogenes* treated with CHEO.

Table 2
The analysis of *L. monocytogenes* cell membrane permeability after CHEO treatment.

Parameter	Control	CHEO
Adsorption rate (%)	3.61 ± 0.032 [a]	4.35 ± 0.043 [b]
OD_{260}	0.126 ± 0.011 [a]	0.290 ± 0.024 [b]
DNA concentration (μg/mL)	7.698 ± 0.53 [a]	2.034 ± 0.12 [b]
ATP bioluminescence (RLU)	4906 ± 324 [a]	754 ± 58 [b]
Protein concentration (μg/mL)	238.1 ± 6.5 [a]	71.4 ± 3.6 [b]
Electrical conductivity (mS/cm)	0.248 ± 0.017 [a]	0.293 ± 0.021 [b]
Surface Zeta potential (mV)	−19.3 ± 0.4 [a]	−29.7 ± 0.3 [b]
Cytoplasmic membrane permeability ($OD_{405\ nm}$)	1.527 ± 0.025 [a]	1.613 ± 0.032 [b]

Values are expressed as mean ± SD.
a–b Different superscripts within the same row indicate significant difference ($P < 0.05$).

consistent with the result of TEM analysis. The increase of surface Zeta potential showed the cells treated with CHEO had an agglutinated trend and thus accelerated the death of bacteria. The electrical conductivity and adsorption rate of *L. monocytogenes* was significantly increased compared with the control, implying that the electrolytes leaked out as a result of the damage of cell membrane. The raise of optical densities (OD) value at 260 nm and 405 nm indicated that the cytoplasmic membrane permeability of *L. monocytogenes* was increased by CHEO. The study of Holle et al. (2012) suggested that the hydrophobicity of essential oils and their components played an important role, causing the active substances accumulated on cell membranes. Then, the structures of cell membranes were destroyed, leading to the increase of permeability. In this study, the main components of CHEO were alcohols, olefins and ketones, belonging to the active ingredients which have the ability to influence cell membrane. But the action site of essential oil on cell membrane is still unknown.

In addition, Arkoun et al. (2017a) provided the evidences that chitosan released from nanofibers have the function of perforator towards bacterial cell membrane. The results indicated proteins and DNA was induced to leak out as chitosan interacted with the negatively charged bacterial cell membrane. The antibacterial mechanism was similar to the mechanism of essential oils. According to these findings, the antibacterial mechanism of CS/NF against *L. monocytogenes* was explored in the next study.

Table 4
The superpose rate of CHEO to representative inhibitor.

Inhibitor	Respiratory rate R_2/ μmol O_2·(g·min)$^{-1}$	Superpose rate $D_R = (R_1\text{-}R_2)/R_1$/%
CHEO	0.3125 ± 0.0271	–
CHEO + Iodoacetic acid	0.4375 ± 0.0153	22.22 ± 0.81 [a]
CHEO + Malonic acid	0.3750 ± 0.0169	30.23 ± 0.54 [b]
CHEO + Trisodium phosphate dodecahydrate	0.3875 ± 0.0127	34.04 ± 0.22 [c]

Values are expressed as mean ± SD.
The concentration of CHEO was ½MIC in the table.
[a–b]Different superscripts within the same row indicate significant difference ($P < 0.05$).

3.1.5. Effects of CHEO on respiratory metabolism of L. monocytogenes

Table 3 exhibited the respiratory inhibition rate I_R of three typical inhibitors and CHEO in the *L. monocytogenes*. Among the three inhibitions, rate of inhibition in malonic acid (22.10%) was high. Obviously, the inhibitory rate of CHEO (54.71%) was higher than all the three inhibitors ($P < 0.05$). The obtained respiratory superpose rate (D_R) (Table 3) was used to determine the way in which the CHEO inhibited respiratory metabolism of *L. monocytogenes*. The three typical respiratory inhibitors, iodoacetic acid, malonic acid and trisodium phosphate dodecahydrate are corresponding to three pathways in glucose decomposition of microbial, they are EMP pathway, tricarboxylic acid (TCA) cycle and pentose phosphate (HMP) pathway. When the superpose rate is smaller, the potential synergistic effect is weaker between bacteriostasis and the typical inhibitor, indicating that the bacteriostatic agent may be have the same respiratory metabolic pathway with the typical respiratory inhibitor. The results were seen in Table 4,

Table 3
Inhibiting rate of the representative inhibitor and CHEO to *L. monocytogenes*.

Inhibitor	Concentration/mg/mL	Respiratory rate R_0/μmol O_2·(g·min)$^{-1}$	Respiratory rate R_1/μmol O_2·(g·min)$^{-1}$	Inhibiting rate I_R/%
Iodoacetic acid	0.5	0.69 ± 0.018	0.5625 ± 0.0236	18.48 ± 0.26 [b]
Malonic acid	0.5	0.69 ± 0.018	0.5375 ± 0.0218	22.10 ± 0.85 [c]
Trisodium phosphate dodecahydrate	0.5	0.69 ± 0.018	0.5875 ± 0.0252	14.86 ± 0.16 [a]
CHEO	2.5	0.69 ± 0.018	0.3125 ± 0.0286	54.71 ± 0.16 [d]

Values are expressed as mean ± SD.
[a–b]Different superscripts within the same row indicate significant difference ($P < 0.05$).

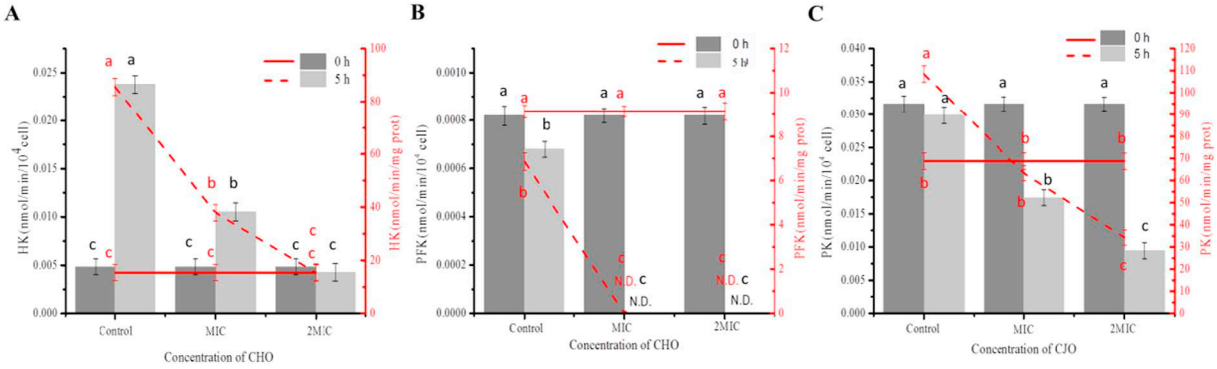

Fig. 2. The activity of enzymes in the reactions: (A) the activity of HK, (B) the activity of PFK, and (C) the activity of PK.

the superpose rate between iodoacetic acid and CHEO (22.22%) was smallest ($P < 0.05$) which implying that EMP pathway was the main way for CHEO to inhibit respiratory metabolism of *L. monocytogenes*.

3.1.6. Effects of CHEO on enzyme activities in EMP pathway

There are three irreversible reactions which were catalyzed by three enzymes, including HK, PFK and PK, respectively. Due to the irreversibility of the reactions, the activity of the enzymes could be used to investigate the effect of CHEO on EMP pathway. The activities of HK and PK were higher than that at 0 h after treated with CHEO for 5 h, while PFK was lower. However, the common point was that the activities of three enzymes were reduced all compared with the control after 5 treatments (Fig. 2A, B and C). The result was indicated that the CHEO had negative effect on the respiratory metabolism of *L. monocytogenes* through EMP pathway (Clara et al., 2016). The similar results were presented in Lin et al., 2018, which illustrated the respiratory metabolism of *L. monocytogenes* was also inhibited by ε-poly-lysine.

3.2. Characterization of the nanofibers

3.2.1. SEM analysis

The representative SEM images of CS/NF and CHEO/CS/NF were depicted and compared in Fig. 3. The diameters of CS/NF have a concentrate range (50–250 nm). As can be seen, the average diameter of the nanofibers was slightly larger when CHEO was loaded, which indicated that CHEO was successfully embedded into nanofibers. Furthermore, the images showed the CS/NF and CHEO/CS/NF were continuous, smooth and well distributed, which was consistent with the morphology reported previously (Rieger, 2013). However, the average fiber diameters (161 nm) in this work differed from that (52 nm) found by Rieger and Schiffman (2014). This was possibly because of different loading concentrations of PEO and CS in nanofibers.

3.2.2. AFM analysis

AFM images were obtained to evaluate the changes of the surface morphology between CS/NF and CHEO/CS/NF (Fig. 4A and B). Different angles of CS/NF and CHEO/CS/NF images were depicted. The average roughness values for CS/NF were lower than CHEO/CS/NF which was ranged from 73.9 to 242.3 nm and 105 to 389.2 nm respectively (Honarvar et al., 2017). It can be visually seen from the two-dimensional diagram that the diameter of CS/NF was smaller than CHEO/CS/NF under the same scale. The three-dimensional morphology showed that the nanofibers had high surface roughness as a result of the random ejection in electrospinning process. The result further verified that the CHEO was encapsulated into chitosan nanofibers.

3.2.3. Physical properties of the nanofibers

The differences between CS/NF and CHEO/CS/NF of thickness, moisture content, water solubility and Transparency were shown in Table 5. The thickness was 0.05 mm and 0.07 mm of CS/NF and CHEO/CS/NF, respectively. Besides, moisture content enhanced from 14.82% to 15.38% ($P < 0.05$). However, water solubility was decreased from 61.27% to 56.48% ($P < 0.05$), when CHEO was hydrophobic.

3.3. The release rate of nanofibers

The release rate of CHEO from the nanofibers was investigated using GC–MS. The experiments were conducted at the cultured temperature of 4 °C, 12 °C, and 25 °C during 15 days storage (Fig. 5). In the result, different degrees of leakage of encapsulated CHEO in nanofibers were observed. The cumulative release rates of CHEO was 43.98%, 55.43%, 62.45% corresponding to respective temperature (4 °C, 12 °C, and 25 °C). The results demonstrated that the CHEO was slowly release out and completely last for 15 days. Obviously, when the temperature increased, the release rate was also increased. The main reason was that a relative higher temperature can cause the increase of the diffusion coefficient of essential oil molecules.

3.4. Antibacterial application of CHEO/CS/NF on beef in vitro

In order to evaluate the antibacterial efficacy of nanofibers effects in food packaging, the CHEO/CS/NF was applied on beef against *L. monocytogenes* by using a plate colony-counting method. The results were shown in Fig. 6. As compared with the control, the population of

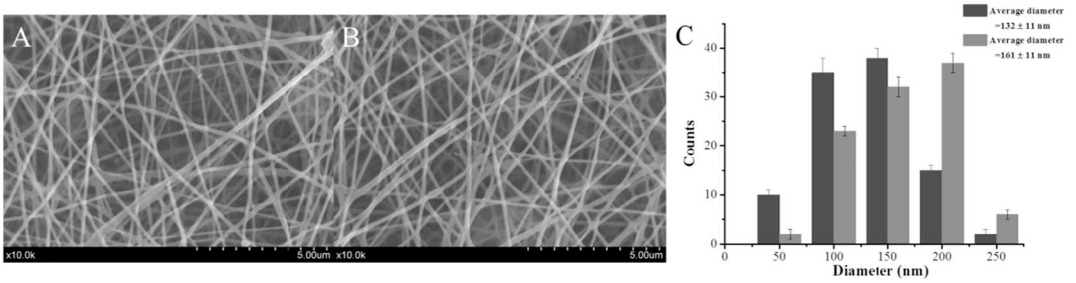

Fig. 3. SEM images and fiber diameter distributions with average diameters of the nanofibers: (A) CS/NF, (B) CHEO/CS/NF, (C) fiber diameter distributions.

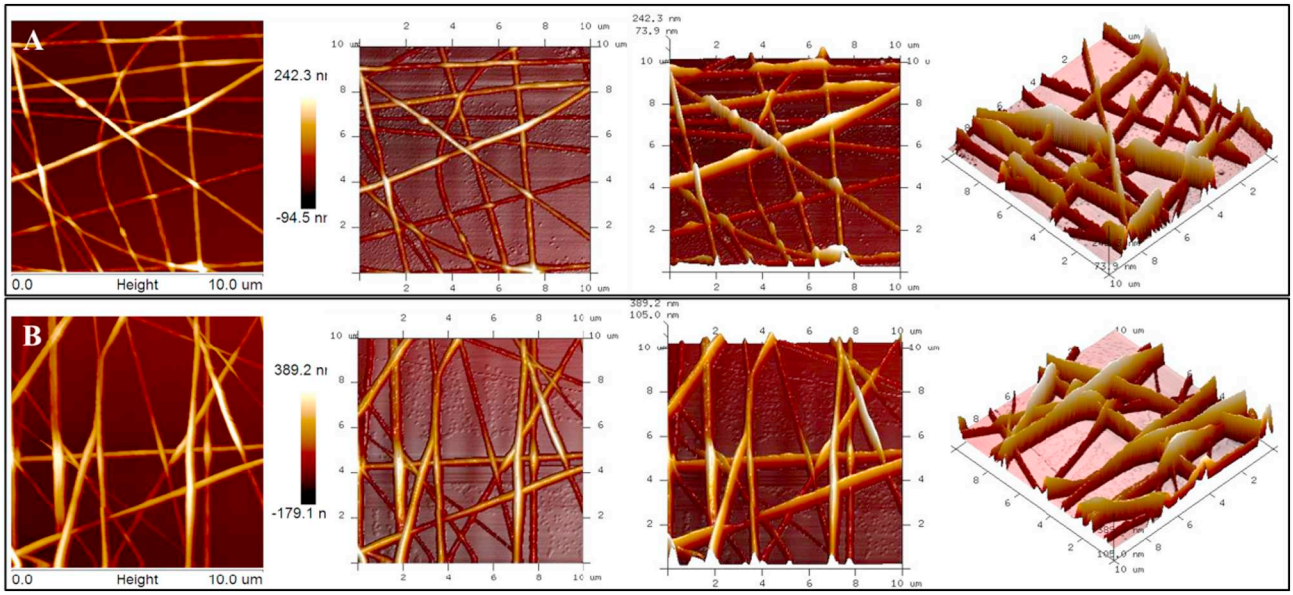

Fig. 4. AFM images of (A) CS/NF, (B) CHEO/CS/NF.

Table 5
Physical properties of the nanofibers.

Parameter	CS/NF	CHEO/CS/NF
Thickness (mm)	0.05 ± 0.011 [a]	0.07 ± 0.009 [b]
Moisture content (%)	14.82 ± 0.13 [a]	15.38 ± 0.16 [b]
Water solubility (%)	61.27 ± 1.65 [a]	56.48 ± 1.26 [b]
T (%/mm)	43.30 ± 0.94 [a]	40.25 ± 0.81 [b]

Values are expressed as mean ± SD.
[a–b]Different superscripts within the same row indicate significant difference ($P < 0.05$).

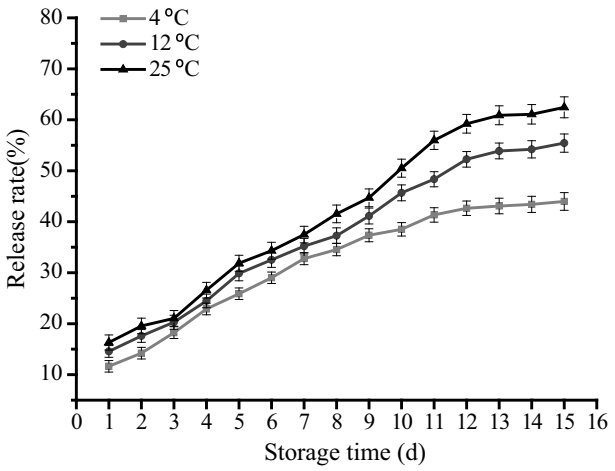

Fig. 5. Release rate of CHEO/CS/NF at 4 °C, 12 °C and 25 °C.

bacteria had a decrease of 85.71%, 81.95%, and 62.16% after treated with CS/NF, and 97.99%, 97.86%, 90.32% after treated with CHEO/CS/NF at the three temperatures at 24 h. Furthermore, 99.91%, 99.97%, and 99.85% reduction in population of *L. monocytogenes* was also observed, respectively, after packing with CHEO/CS/NF for 7 days at 4 °C, 12 °C, and 25 °C. Arkoun et al. (2017b) also demonstrated the chitosan nanofibers had the ability to eradicate 92% of bacterial population in contaminated beef samples. It was apparently that the growth of *L. monocytogenes* was rather slower at the incubation temperature of 4 °C and 12 °C than 25 °C. This might attributed to the optimum growth temperature of bacteria.

The result was proved that the CHEO/CS/NF had the ability to inhibit the growth of *L. monocytogenes* on beef, and the antibacterial efficiency was better than beef packed with CS/NF. Hence, CHEO/CS/NF was potential in beef products packaging for consideration of food safety.

3.5. The TBARS value

Fat oxidation was a major cause of deterioration in the quality of meat and meat products during storage, resulting in serious loss of flavor and nutritional value (fat acids and fat-soluble vitamins). The changes of TBARS value for the beef samples were presented in Fig. 7. Initially, the TBARS value was 0.283 mg malondialdehyde (MDA)/kg which indicated a low level lipid oxidation. After 4 days treatment with the nanofibers, the increased value of the treated beef was apparently smaller than the control at the tested temperature. During the storage time, the increase in TBARS value was related to the accumulation of lipid oxidation products (Chouliara et al., 2007). The TBARS value of the treated beef samples (0.408 mg MDA/kg) was lower than untreated (0.543 mg MDA/kg) after 12 days at 4 °C ($P < 0.05$). However, there were no obvious difference between the TBARS value of the control and CS/NF ($P > 0.05$). The results indicated that CHEO/CS/NF could slow down the rate of lipid oxidation and maintain freshness thus prolong shelf-life. The phenomenon was in agreement with the conclusion that lower lipid oxidation was owing to the presence of antioxidant components (Menon and Padmakumari, 2005), as CHEO contained the components which could contribute hydrogen atoms to electrons and stabilize free radicals (Redondo-Cuevas et al., 2017), such as β-Selinene, 3-ethylidence-1-methylcyclopentene, α-Curcumene. Furthermore, the similar phenomenon was observed at 12 °C and 25 °C.

3.6. The pH value

The differences of changed pH values were depicted in Fig. 8. The initial pH value of the beef sample was 5.45. The pH value was decreased due to a certain degree of postmortem glycolysis of fresh beef, during the first 2 days at 4 °C. Then, the pH of all the samples were gradually increased during storage which was attributed to the degradation of proteins and the accumulation of ammonia released from microbial (Soultos et al., 2008). On the 10th day, the pH value of the

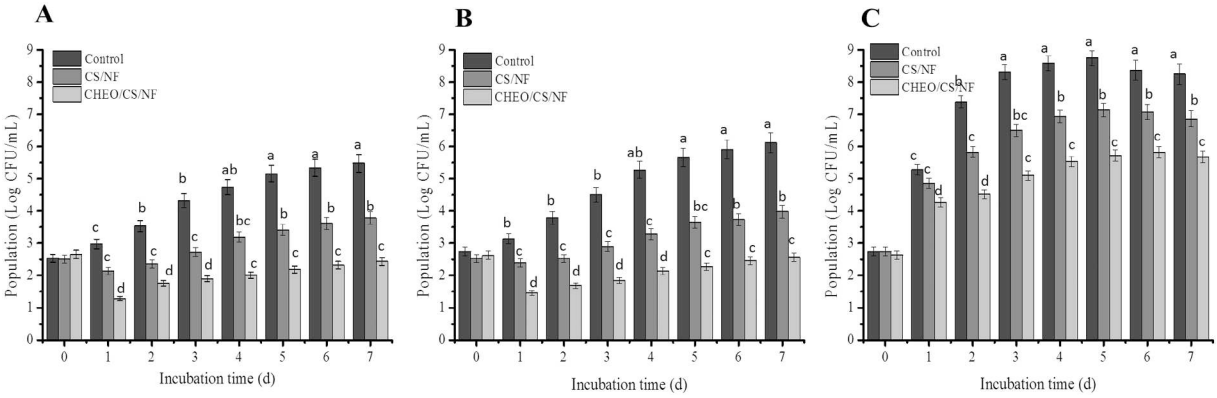

Fig. 6. The inhibitory activity of the nanofibers against *L. monocytogenes* on beef at 4 °C (A), 12 °C (B), and 25 °C (C).

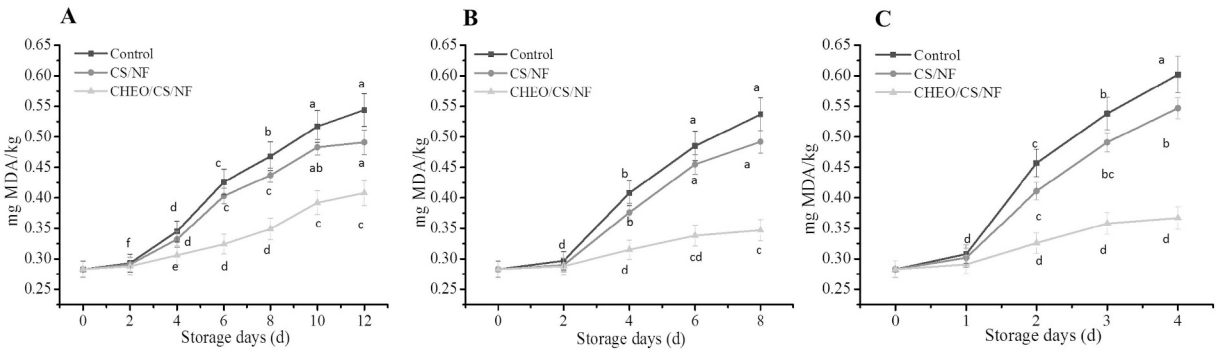

Fig. 7. Changes in TBARS values in beef samples during storage at 4 °C (A) 12 °C (B), and 25 °C (C).

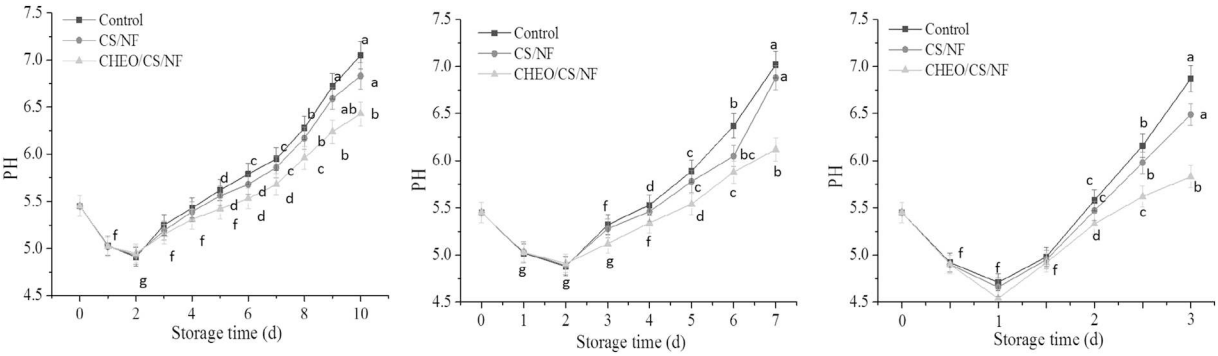

Fig. 8. Changes in pH values in beef samples during storage at 4 °C (A) 12 °C (B), and 25 °C (C).

control was 7.05, while the beef treated with CS/NF and CHEO/CS/NF was 6.83 ($P > 0.05$) and 6.43 stored at 4 °C ($P < 0.05$). The results were suggested that CHEO/CS/NF had a better effect on delaying PH value growth than CS/NF due to the action of CHEO. Besides, the similar phenomenon was observed at 12 °C and 25 °C, either. PH value was related to microbial proliferation and shelf life as reported by Holmer et al. (2009). The microbial proliferation will be accelerated and the shelf-life will be shortened with the increase of pH value. In other words, the CHEO/CS/NF packaging can maintain the quality of beef via keeping pH value low.

3.7. Color and texture evaluation

A comparison of color and texture between the control and the treated beef samples at the temperature of 4 °C and 25 °C was performed in this study (Table 6 and Table 7). The color of meat was determined by the physico-chemical state of myoglobin, containing purple reduced myoglobin (Mb), red oxymyoglobin (MbO_2) and brown metmyoglobin (MetMb) (Abril et al., 2001). According to Table 6, the color values including L*, a* and b* values, adhesiveness, resilience, and springiness were altered in the treatment group. Conversely, the hardness, cohesion, gumminess and chewiness were not changed. The changes of L*, a* and b* values were due to the difference of CHEO/CS/NF color on the surface of treated meat.

4. Conclusions

Based on above results, the CHEO exhibited high antibacterial activity against *L. monocytogenes* through destroying bacterial cell membrane. The leakage of intracellular macromolecule and losses of 260_{nm}

Table 6
Color and texture of beef samples after treatment at 4 °C for 7 days.

Parameters		0 d	7 d (control)	7 d (treatment)
Color	L*	38.26 ± 0.37 [b]	35.47 ± 0.34 [a]	41.78 ± 0.35 [c]
	a*	23.50 ± 0.25 [a]	32.18 ± 0.32 [c]	28.23 ± 0.28 [b]
	b*	9.45 ± 0.42 [a]	12.66 ± 0.46 [c]	11.39 ± 0.43 [b]
Textural	Hardness (Kg)	16.72 ± 0.56 [a]	17.52 ± 0.59 [a]	17.35 ± 0.55 [a]
	Adhesiveness (g. *sec*)	−73.80 ± 0.41 [a]	−56.16 ± 0.36 [c]	−58.41 ± 0.39 [b]
	Resilience (%)	34.18 ± 0.23 [c]	31.86 ± 0.19[a]	32.34 ± 0.24 [b]
	Cohesion	0.67 ± 0.13 [a]	0.79 ± 0.17 [a]	0.73 ± 0.14 [a]
	Springiness (%)	85.46 ± 0.63 [c]	52.58 ± 0.57 [a]	56.97 ± 0.60 [b]
	Gumminess	5.92 ± 0.21 [a]	6.14 ± 0.22 [a]	6.09 ± 0.18 [a]
	Chewiness	7.84 ± 0.15 [b]	5.65 ± 0.14 [a]	5.93 ± 0.11 [a]

Values are expressed as mean ± SD.
[a–b]Different superscripts within the same row indicate significant difference ($P<0.05$).

Table 7
Color and texture of beef samples after treatment at 25 °C for 3 days.

Parameters		0 d	3 d (control)	3 d (treatment)
Color	L*	38.26 ± 0.34 [b]	34.65 ± 0.32 [a]	40.96 ± 0.37 [c]
	a*	23.50 ± 0.28 [a]	33.14 ± 0.33 [c]	29.52 ± 0.31 [b]
	b*	9.45 ± 0.39 [a]	12.63 ± 0.41 [c]	11.23 ± 0.35 [b]
Textural	Hardness (Kg)	16.72 ± 0.46 [a]	18.22 ± 0.54 [a]	17.60 ± 0.50 [a]
	Adhesiveness (g. sec)	−73.80 ± 0.22 [c]	−46.38 ± 0.27 [a]	−48.49 ± 0.25 [b]
	Resilience (%)	34.18 ± 0.57 [c]	29.74 ± 0.53 [a]	31.56 ± 0.61 [b]
	Cohesion	0.67 ± 0.15 [a]	0.81 ± 0.18 [a]	0.77 ± 0.13 [a]
	Springiness (%)	85.46 ± 0.72 [c]	49.68 ± 0.69 [a]	51.19 ± 0.73 [b]
	Gumminess	5.92 ± 0.23 [a]	6.31 ± 0.19 [a]	6.23 ± 0.24 [a]
	Chewiness	7.84 ± 0.30 [b]	6.94 ± 0.25 [a]	6.58 ± 0.26 [a]

Values are expressed as mean ± SD.
[a–c]Different superscripts within the same row indicate significant difference ($P<0.05$).

absorbing materials resulted in the death of bacteria. Another mechanism of the CHEO against *L. monocytogenes* was the inhibition of respiratory metabolism through EMP pathway. Due to the complex nature of CHEO, other processes may be inhibited such as protein expression and topoisomerase activity. These possibilities will be further investigated in the later studies. Moreover, the electrospun of CHEO/CS/NF was successfully fabricated under the optimal conditions. The practical application in beef exhibited that the CHEO/CS/NF possessed long-term anti-*L. monocytogenes* effect during 7-day storage. Importantly, the nanofibers have no impact on the quality of beef on the basis of the results of color and texture evaluation. Briefly, along with the slow release and antibacterial ability of CHEO, CHEO/CS/NF could effectively prolong the shelf-life of beef, thus having a broad prospect in food packaging field.

Acknowledgement

The authors acknowledge the financial support from Natural Science Foundation of Jiangsu Province, China (grant no. BK20170070), Jiangsu Province Foundation for talents of six key industries, China (grant no. NY-013), Profession scientific research special item of agricultural public welfare, China (grant no. 201403039) and Jiangsu University Research Fund, China (grant no. 11JDG050).

Competing interests

None declared.

Ethical approval

Not required.

References

Abril, M., Campo, M.M., Onenç, A., Sañudo, C., Albertí, P., Negueruela, A.I., 2001. Beef colour evolution as a function of ultimate pH. Meat Sci. 58, 69–78.
Alippilakkotte, S., Sreejith, L., 2018. Benign route for the modification and characterization of poly (lactic acid) (PLA) scaffolds for medicinal application. J. Appl. Polym. Sci. 135, 46056.
Ammar, H.O., El-Nahhas, S.A., Ghorab, M.M., Salama, A.H., 2012. Chitosan/cyclodextrin nanoparticles as drug delivery system. J. Incl. Phenom. Macrocycl. Chem. 72, 127–136.
Arkoun, M., Daigle, F., Heuzey, M.C., Ajji, A., 2017a. Antibacterial electrospun chitosan-based nanofibers: a bacterial membrane perforator. Food Sci. Nutr. 5, 865–874.
Arkoun, M., Daigle, F., Heuzey, M.C., Ajji, A., 2017b. Mechanism of action of electrospun chitosan-based nanofibers against meat spoilage and pathogenic bacteria. Molecules 22, 585.
Arokiyaraj, S., Arasu, M.V., Vincent, S., Prakash, N.U., Choi, S.H., Oh, Y.K., Chio, K.C., Kim, K.H., 2014. Rapid green synthesis of silver nanoparticles from chrysanthemum indicum l and its antibacterial and cytotoxic effects: an in vitro study. Int. J. Nanomedicine 9, 379–388.
Benker, H., 1985. Functional compartmentation of glycolytic versus oxidative metabolism in isolated rabbit heart. J. Clin. Invest. 75, 436.
Brown, T.D., Dalton, P.D., Hutmacher, D.W., 2016. Melt electrospinning today: an opportune time for an emerging polymer process. Prog. Polym. Sci. 56, 116–166.
Caredda, A., Marongiu, B., Silvia Porcedda, A., Soro, C., 2002. Supercritical carbon dioxide extraction and characterization of *Laurus nobilis* essential oil. J. Agric. Food Chem. 50, 1492–1496.
Catanzano, O., Straccia, M.C., Miro, A., Ungaro, F., Romano, I., Mazzarella, G., Santagata, G., Quaglia, F., Laurienzo, P., Malinconico, M., 2015. Spray-by-spray in situ cross-linking alginate hydrogels delivering a tea tree oil microemulsion. Eur. J. Pharm. Sci. 66, 20–28.
Chouliara, E., Karatapanis, A., Savvaidis, I.N., Kontominas, M.G., 2007. Combined effect of oregano essential oil and modified atmosphere packaging on shelf-life extension of fresh chicken breast meat, stored at 4 degrees C. Food Microbiol. 24, 607–617.
Clara, R., Langhans, W., Mansouri, A., 2016. Oleic acid stimulates glucagon-like peptide-1 release from enteroendocrine cells by modulating cell respiration and glycolysis. Metabolism 65, 8–17.
Cui, H.Y., Li, W., Lin, L., 2016. Bacterial protease-triggered clove oil release from proteoliposomes against *S. aureus* biofilms on dried soybean curd. RSC Adv. 6, 34833–34840.
Cui, H.Y., Yuan, L., Li, W., Lin, L., 2017. Edible films incorporated with chitosan and *Artemisia annua* oil nanoliposomes for inactivation of *E. coli* O157:H7 on cherry

tomatoes. Int. J. Food Sci. Technol. 52, 687–698.
Cui, H.Y., Bai, M., Sun, Y.H., Mohamed, A.S., Abdel, S., Lin, L., 2018. Antibacterial activity and mechanism of Chuzhou chrysanthemum essential oil. J. Funct. Foods 48, 159–166.
Gutierrez, J., Barry-Ryan, C., Bourke, P., 2008. The antimicrobial efficacy of plant essential oil combinations and interactions with food ingredients. Int. J. Food Microbiol. 124, 91–97.
Haider, S., Park, S.Y., 2009. Preparation of the electrospun chitosan nanofibers and their applications to the adsorption of Cu (ii) and Pb (ii) ions from an aqueous solution. J. Membr. Sci. 328, 90–96.
Holle, A.V., Machado, M.D., Soares, E.V., 2012. Flocculation in ale brewing strains of saccharomyces cerevisiae: re-evaluation of the role of cell surface charge and hydrophobicity. Appl. Microbiol. Biotechnol. 93, 1221–1229.
Holmer, S.F., Mckeith, R.O., Boler, D.D., Dilger, A.C., Eggert, J.M., Petry, D.B., Mckeith, F.K., Jones, K.L., Killefer, J., 2009. The effect of ph on shelf-life of pork during aging and simulated retail display. Meat Sci. 82, 86–93.
Honarvar, Z., Farhoodi, M., Khani, M.R., Mohammadi, A., Shokri, B., Ferdowsi, R., Shojaee-Aliabadi, S., 2017. Application of cold plasma to develop carboxymethyl cellulose-coated polypropylene films containing essential oil. Carbohydr. Polym. 176, 1–10.
Huang, Z.M., Zhang, Y.Z., Kotaki, M., Ramakrishna, S., 2003. A review on polymer nanofibers by electrospinning and their applications in nanocomposites. Compos. Sci. Technol. 63, 2223–2253.
Khallouki, F., Hmamouchi, M., Younos, C., Soulimani, R., Bessiere, J.M., Essassi, E.M., 2000. Antibacterial and molluscicidal activities of the essential oil of chrysanthemum viscidehirtum. Fitoterapia 71, 544–546.
Krauland, A.H., Alonso, M.J., 2007. Chitosan/cyclodextrin nanoparticles as macromolecular drug delivery system. Int. J. Pharm. 340, 134–142.
Lasheen, M.R., El-Sherif, I.Y., Tawfik, M.E., El-Wakeel, S.T., El-Shahat, M.F., 2016. Preparation and adsorption properties of nano magnetite chitosan films for heavy metal ions from aqueous solution. Mater. Res. Bull. 80, 344–350.
Lin, L., Zhang, X.J., Zhao, C.T., Cui, H.Y., 2016. Liposome containing nutmeg oil as the targeted preservative against *Listeria monocytogenes* in dumplings. RSC Adv. 6, 978–986.
Lin, L., Dai, Y.J., Cui, H.Y., 2017. Antibacterial poly(ethylene oxide) electrospun nanofibers containing cinnamon essential oil/beta-cyclodextrin proteoliposomes. Carbohydr. Polym. 178, 131–140.
Lin, L., Gu, Y.L., Li, C.Z., Vittayapadung, S., Cui, H.Y., 2018. Antibacterial mechanism of ε-poly-lysine against listeria monocytogenes, and its application on cheese. Food Control 91, 76–84.
Menon, A.N., Padmakumari, K.P., 2005. Studies on essential oil composition of cultivars of black pepper (*Piper nigrum* L.) - IV. J. Essent. Oil Res. 17, 153–155.
Miao, J., Peng, W., Liu, G., Chen, Y., Chen, F., Cao, Y., 2015. Biopreservative effect of the natural antimicrobial substance from *Lactobacillus paracasei*, subsp. *tolerans*, fx-6 on fresh pork during chilled storage. Food Control 56, 53–56.
Pesavento, G., Calonico, C., Bilia, A.R., Barnabei, M., Calesini, F., Addona, R., Mencarelli, L., Carmagnini, L., Di Martino, M.C., Lo Nostro, A., 2015. Antibacterial activity of Oregano, Rosmarinus and Thymus essential oils against *Staphylococcus aureus*, and *Listeria monocytogenes* in beef meatballs. Food Control 54, 188–199.
Redondo-Cuevas, L., Castellano, G., Raikos, V., 2017. Natural antioxidants from herbs and spices improve the oxidative stability and frying performance of vegetable oils. Int. J. Food Sci. Technol. 52, 2422–2428.
Rieger, K.A., 2013. Designing electrospun nanofiber mats to promote wound healing-a review. J. Mater. Chem. 1, 4531–4541.
Rieger, K.A., Schiffman, J.D., 2014. Electrospinning an essential oil: cinnamaldehyde enhances the antimicrobial efficacy of chitosan/poly (ethylene oxide) nanofibers. Carbohydr. Polym. 113, 561–568.
Samira, S., Thuanchew Tan, T.C., Azhar, M.E., 2014. Effect of ribose-induced maillard reaction on physical and mechanical properties of bovine gelatin films prepared by oven drying. Int. Food Res. J. 21, 269–276.
Schmidt, M.M., Dringen, R., 2009. Differential effects of iodoacetamide and iodoacetate on glycolysis and glutathione metabolism of cultured astrocytes. Front. Neuroenerg. 1 (1).
Shojaeealiabadi, S., Hosseini, H., Mohammadifar, M.A., Mohammadi, A., Ghasemlou, M., Ojagh, S.M., Hoseini, S.M., Khaskar, R., 2013. Characterization of antioxidant-antimicrobial κ-carrageenan films containing *Satureja hortensis* essential oil. Int. J. Biol. Macromol. 52, 116–124.
Soultos, N., Tzikas, Z., Abrahim, A., Georgantelis, D., Ambrosiadis, I., 2008. Chitosan effects on quality properties of Greek style fresh pork sausages. Meat Sci. 80, 1150–1156.
Tsigarida, E., Skandamis, P., Nychas, G.J.E., 2010. Behaviour of *Listeria monocytogenes*, and autochthonous flora on meat stored under aerobic, vacuum and modified atmosphere packaging conditions with or without the presence of oregano essential oil at 5 °C. Appl. Microbiol. 89, 901–909.
Ubonrat, S., Brucer, H., 2010. Physical properties and antioxidant activity of an active film from chitosan incorporated with green tea extract. Food Hydrocoll. 24, 770–775.
Vodnar, C.V., 2012. Inhibition of *Listeria monocytogenes* ATCC 19115 on ham steak by tea bioactive compounds incorporated into chitosan-coated plastic films. Chem. Cent. J. 6, 74.
Wemmenhove, E., Wells-Bennik, M.H., Stara, A., Hooijdonk, A.C., Zwietering, M.H., 2016. How NaCl and water content determine water activity during ripening of Gouda cheese, and the predicted effect on inhibition of *Listeria monocytogenes*. J. Dairy Sci. 99, 5192–5201.
Zhang, J., Wang, Y., Pan, D.D., Cao, J.X., Shao, X.F., Chen, Y.J., Sun, Y.Y., Ou, C.R., 2016. Effect of black pepper essential oil on the quality of fresh pork during storage. Meat Sci. 117, 130–136.